Activation of nanoflows for fuel cells

Z. Insepov,[1,2] Robert J. Miller[3]
[1]Argonne National Laboratory, 9700 South Cass Ave., Argonne, IL 60439
[2]Purdue University; 400 Central Drive, West Lafayette, IN 47907
[3] Clerisity LLC, 14 Oakwood Pl., Delmar, NY 12054

ABSTRACT

Propagation of Rayleigh traveling waves on a nanotube surface activates a macroscopic flow of the gas (or gases) that depends critically on the atomic mass of the gas. Our molecular dynamics simulations show that the surface waves are capable of actuating significant macroscopic flows of atomic and molecular hydrogen, helium, and a mixture of both gases both inside and outside carbon nanotubes. In addition, our simulations predict a new "nanoseparation" effect when a nanotube is filled with a mixture of two gases with different masses or placed inside a volume filled with a mixture of several gases with different masses. The mass selectivity of the nanopumping can be used to develop a highly selective filter for various gases. Gas flow rates, pumping, and separation efficiencies were calculated at various wave frequencies and phase velocities of the surface waves. The nanopumping effect was analyzed for its applicability to actuate nanofluids into fuel cells through carbon nanotubes.

INTRODUCTION

A significant engineering problem arises in the development of a novel solid-state air movement technology that brings high flux rates with lower parasitic power requirements in micro fuel cell systems. Current microelectronics fabrication processes for micro fuel cell systems are inadequate to provide high volumetric densities at attractive prices. These inadequacies are associated predominantly with balance-of-plant components. More specifically, no viable solid-state air pumps can be easily integrated into microfabricated flow fields for fuel cells. More generally, the parasitic power draw of typical air pumps is about 50% electronic driver efficiency and 50% power to move the motor. As such, today motor-driven air delivery uses about 15% to 20% of the system power available from micro fuel cells. In addition, the cost of such pumps is on the order of $20/watt or more, about ten times higher than the projected market will likely accept. Typical manufacturing processes are molding with automated assembly of discrete pumps if volumes are high. Most of the costs are associated with the motor and bearings in these small systems.

Clearly needed are robust solid-state micropumps for air delivery that achieve cost effectiveness by removing the costly parts of typical motor-driven pumps. Equally needed is a

method for integrating such pumps into known microfabrication processes. These objectives can be achieved independently or together. Special emphasis is placed on new physics that leverages unique nanoscale materials properties or novel approaches to move air. The independent goals are to (1) provide air delivery at a constant 400 mA/cm^2 flux while requiring less than 5% of the generated power and (2) be easily integrated into the stack without adding significantly to the system volume.

More specifically, a novel nanomechanical pump (nanopump) is desirable that will be capable of pumping gases and liquids at the nanoscale, through channels with diameters as small as 1–10 nm.

Such nanopumps will be important devices in cell biology for facilitation, acceleration, and control of the ion exchange into and out of a cell; in medicine, for selective drag delivery in a human body; in energy technology, for hydrogen storage in carbon nanotubes and for hydrogen transport through them. Here, we explain the main principle of our technique as it is applied for hydrogen storage and transport in carbon nanotubes.

1.1 Related Work

Carbon nanotubes with the diameters of 1–50 nm would be an ideal nanopumping device. As yet, however, there have been no indications how to force such nanotubes to work as nanopumps.

The outcome of many theoretical and experimental efforts to date specifies that carbon nanostructures could be considered as a promising path to future hydrogen storage fuel cells. However, further progress is essential in both theory and experiment in order to move to an engineering stage of using a carbon nanotube as a prospective fuel cell.

Dillon et al. have determined that the hydrogen storage in single-walled nanotubes (SWNTs) could be as big as 5–10 wt% at an ambient temperature of 133 K and pressure of 300 torr [1].

Liu et al. have found that by increasing the purity of the nanostructures, the filling result could be about 4.2 wt% at a pressure of 10 MPa and at room temperature [2]. Multiwalled nanotubes (MWNTs) could store more hydrogen than could SWNTs [3].

Ye et al. have reported the hydrogen storage of 8 wt% at 40 atm and 80 K on purified laser-generated crystalline ropes of SWNTs [4]. However, the hydrogen capacities on the laser-generated tubes were low at room temperature and pressures below 1 atm.

The maximum absorption capacity of 7 wt% was observed by Dillon et al. [5,6] on the laser-generated SWNTs when they were processed with a high-power ultrasonic cutting procedure (sonication) that incorporates a $TiAl_{0.1}V_{0.04}$ alloy due to decomposition of ultrasonic probe. The sonication procedure was applied to cut long carbon chains but was not studied itself, and the increase of the hydrogen was attributed to the presence of the alloy [6]. The authors also pointed to the difficulties of obtaining high-surface-area, "activated" carbon adsorbents with small pore sizes and narrow pore-size distributions in SWNTs.

More than 50% of the total pore number should be considered as macropores, with the diameters more that 40 Å. Macropores participate only in monolayer type hydrogen adsorption and therefore are not useful for ambient-temperature hydrogen storage. None of the experimental results were confirmed by independent research groups [6].

Some theoretical studies predict the capacity of 4–14 wt%. However, most recent theoretical papers [7–10] predict negligible hydrogen adsorption to the carbon nanotube at room temperature.

Experimental studies of hydrogen storage in nanostructures have provided a preliminary understanding of the problem. However, theoretical and simulation work on hydrogen storage in nanotubes has not been sufficient. The lack of simulation, in particular, significantly hampers the further development of the fuel cells.

The dynamics of hydrogen filling, phase transitions within the nanotubes, and pumping flow through the nanotubes also have not been studied. Hydrogen has great potential as an energy source and is capable of reducing the U.S. dependence on foreign oil products. Hydrogen can also decrease pollution and greenhouse gas emissions. Fuel cells using hydrogen produced by nuclear energy result in reduced air pollutants and near-zero carbon emissions.

1.2 National Hydrogen Programs

A Hydrogen Fuel Initiative (HFI) was announced in the President's 2003 State of the Union address to accelerate the research, development, and demonstration of technologies for fuel cell vehicles and the hydrogen fuel infrastructure to support them.

In 2006, President Bush announced the Advanced Energy Initiative (AEI), which accelerates R&D of technologies for both transportation and stationary power generation, includes near-term transportation solutions such as plug-in hybrids and ethanol vehicles, and supports the hydrogen R&D efforts that are under way.

Beginning in fiscal year 2004, the HFI increased federal funding for hydrogen and fuel cell research, development, and demonstration (RD&D) to $1.2 billion over five years. With this increase in funding, the HFI accelerated the pace of RD&D efforts focused on achieving specific targets that would enable hydrogen and fuel cell technology readiness in the 2015 timeframe.

The central mission of the current U.S. Department of Energy Hydrogen Program is to research, develop, and validate hydrogen production, delivery, storage, and fuel cell technologies.

2. CHALLENGES FOR HYDROGEN AS AN ENERGY CARRIER

The transition to a clean energy source based on hydrogen will take decades because of the existing technological, economic, and institutional challenges [11].

- The storage for hydrogen vehicles is inadequate to meet the drive expectations (>300 miles).
- The cost of hydrogen is greater than that of gasoline.
- The existing fuel cell system costs are more than those of internal combustion engines.
- The investment risk in developing a hydrogen engine and fuel cells is high.
- The investment risk in developing manufacturing capability for hydrogen and fuel cell technologies is high.
- Uniform model codes and standards to ensure safety and insurability do not exist.
- Local code officials, policy makers, and the general public lack education on hydrogen benefits and on safe handling and use.

Developing hydrogen as a major energy carrier cannot be accomplished by private companies because it requires large investments in research and development, infrastructure, and market acceptance. The success of hydrogen technology requires assistance through government policies until the technologies and the markets mature, in a timeframe of decades. Several breakthrough technologies are necessary:

- Compact, lighter, lower-cost, safe, and efficient higher storage systems
- More durable materials for advanced fuel cells

- Lower-cost methods for producing and delivering hydrogen
- Materials safe for hydrogen use.

In this paper we review published simulation results regarding the nanopumping effect as applied to activated flows of hydrogen. We include some new results (submitted for publication) on activation of a macroscopic flow in a mixture of two gases, with different atomic masses, placed either inside or outside a carbon nanotube. These simulations show that macroscopic flows of atomic and molecular hydrogen, helium, and a mixture of both gases can be successfully activated for both inside and outside a carbon nanotube. They predict a new "nanoseparation" effect consisting of effective separation of two gases. The simulations show that propagation of Rayleigh traveling waves from a gas on a nanotube surface activates a macroscopic flow of the gas (or gases) that depends significantly on the atomic mass of the gas [12]. These results show that the mass-selectivity of the nanopumping effect can be used to develop a highly selective filter for various gases. Gas flow rates and pumping and separation efficiencies were calculated at various wave frequencies and phase velocities of the surface waves.

Areas of interest include highly efficient solid-state air pumps: for example, PZT materials and EWOD approaches, miniaturized O_2 enrichment by pressure swing adsorption, and nanoscale pumping (see [45]).

3. ACTUATION OF GAS FLOW IN NANOTUBES

Actuation of a gas and fluid flow in microcapillaries is of both fundamental and practical interest in the areas of nanorobotics, fine printing at nanoscale, atomic optics, quantum computing, hydrogen energetics, chemical process control, cell biology, medical drug delivery, and molecular medicine [12–21]. Microflow control is important for various industrial and commercial applications: DNA analysis, drug screening, optical display technologies, tunable fiber optic waveguides, thermal management of semiconductor devices and lasers, clinical and forensic analysis, and environmental monitoring [12].

Most of the existing fluidic devices are based on the following physical effects: electro-osmosis, electrohydrodynamics, magnetohydrodynamics, centrifugation, pressure gradient, and modulation of the stresses at the fluid-fluid and fluid-solid interfaces [12].

Molecular dynamics (MD) simulations of some of these phenomena were given in [13–23]. The authors of [13] showed that when the contact angle is large enough, the boundary condition can drastically differ (at a microscopic level) from a "no-slip" condition. Slipping lengths exceeding 30 molecular diameters are obtained for a contact angle of 140°, characteristic of mercury on glass.

Study of fluid flows in narrow channels has become a major area of research since the discovery of nanotubes by Ijima in 1991. The microflow systems include very thin liquid films on solid surfaces [14,15], microfluid arrays [16], inhomogeneous liquid flows in narrow slit-pores [17], flows in micropumps and membranes [12,18], and flows in three-dimensional structures with thousands of microchannels [19].

4. COMPUTER SIMULATION OF FLUID FLOW IN NANOTUBES

Fluid-flow dynamics of gases and liquids in carbon nanotubes was reported in [20–24]. The movement of the walls strongly influences the helium and argon gas flows inside a carbon nanotube [20]. The effect of filling nanotubes with C_{60}, CH_4, and Ne gases on the mechanical properties of the nanotubes was examined in [21]. The authors of [22,23] found that even the smallest nanotubes {7x7} imbibed at an extremely high rate (≤ 800 m/s). The nanoscale imbibition does not obey a Washburn equation applicable to continuum flows. The latter predicts a square root dependence of the imbibition rate on time. However, it is r a complex process showing a linear time dependence on the level of filling [22].

The authors of [23] also found that until a threshold internal pressure is reached inside the liquid, the wetting and filling of the nanotube do not occur. In addition, they predicted that a periodic external pressure applied to liquid generates a discontinuous flow through the nanotube embedded into the liquid [23].

Interaction of fluids with microscopic pores by filling (imbibition) of nanotubes with oil or mercury is of great technological interest [22,23,24]. For example, inorganic nanotubes were successfully integrated with a microfluidic system to create a first nanofluidic device capable of sensing a single DNA molecule [24].

Various methods for atomic pumping through carbon nanotubes were proposed in [26, 27]. In [26], a laser-driven pump for atomic transport through carbon nanotube (CNT) was proposed based on the generation of electric current through the tube, which in turn would move

ions in it by drag forces. A nanopipette concept for dragging metal ions through a multiwalled CNT was experimentally confirmed [27].

Hydrogen adsorption by graphite nanofibers and carbon nanotubes was studied by MD, grand canonical Monte Carlo, and ab initio methods in [28–31]. Liberation of atomic form of hydrogen chemisorbed on carbon materials was discussed in [28,29]. The gas-surface virial coefficient and isosteric heat of adsorption were calculated by classical methods in [28]. A review of experimental and computer simulation results of adsorption of hydrogen on carbon nanotubes and on graphitic nanofibers was given in [29].

Transition metals bound to fullerenes c60 were found to increase hydrogen storage in carbon nanotubes [30]. The binding energy of hydrogen molecule was calculated to be 0.3 eV/H_2, which is an ideal value for use in vehicles. The theoretical maximum retrievable H_2 storage density is 9 wt%.

This hydrogen release process is critical for future hydrogen application in the car industry. Even if the U.S. Department of Energy target of 6.5 wt% of hydrogen storage is reachable, for example, by a chemisorption mechanism, the subsequent liberation of hydrogen by heating will need very high temperatures, thus making this application unrealistic [31]. IN one study [31], ultrasonication of single-walled carbon nanotubes showed an uptake of hydrogen at room temperature; however, the authors attributed this uptake to possible metal contamination during the sonication process.

Contrary to the dense fluid flows in micron- and nanometer-size channels, rarefied gas flows are of interest for future gas pumping. Micro-electromechanical systems and microscale vacuum technology devices are yet another area of applications [32–35].

The rarefied gas flows in a naturally occurring zeolite, clinoptilolite, for a chip-scale, thermal transpiration-based gas pump were studied in [36].

Molecular dynamics and Monte Carlo methods were applied for studying microfluids [14,17,20–25]. Propagation of acoustic waves on metal cylinders and through the carbon nanotubes was discussed in [37–42].

Surface traveling waves can be activated on the nanotube surface in a few ways. One way is to use short laser pulses to generate thermoacoustic waves on a tube [41]. Another way is to send ultrasound waves through the liquid or dense gaseous media to the nanotube [42]. Rayleigh surface waves are activated when a longitudinal wave traveling in a liquid/gas impinges on a

solid surface at an incidence angle equal to the Rayleigh angle θ (where θ = arcsine (C_p/C_s), C_p is the velocity of the incident wave, and C_s is the velocity of the surface wave in the material [42].

Propagation of the specific traveling waves on the dolphin skin surface is discussed in [43,44].

The goal of this paper is to highlight a new high-risk, high-reward science and technology that could achieve transformational results by proving the nanopumping concept and enabling pumping gases at the nanoscale, through nanometer-scale or micrometer-scale channels.

5. SIMULATION MODEL

As an input structure for the molecular dynamics (MD) simulations, coordinates of the zigzag nanotube carbon atoms were generated. The details of our simulations can be obtained elsewhere [45,46]. We placed 128, 256, or 384 gas atoms with four different masses (lighter than or equal to carbon mass) inside the nanotube of 705, 1410, or 2115 carbon atoms with corresponding lengths of 50, 100, and 150 Å. We applied a traveling wave along the nanotube surface.

The gas-separation MD simulation model contained 128 or 256 atoms that were placed inside (or outside) the {15x0} carbon nanotube built of 1,410 carbon atoms. The Rayleigh (traveling) surface waves were generated on the surface of the nanotubes, at various frequencies, amplitudes, and phase velocities. When the gases were placed outside the nanotube, the gas atoms were confined inside an ideally specularly (mirrorlike) reflecting cylinder of a 20 Å diameter.

6. NANOPUMPING

According to our simulation results shown in Fig. 1, the gas atoms inside the nanotube move almost freely, along the ballistic trajectories, and they are easily accelerated to a very high axial velocity, along the direction of the traveling wave as a result of multiple synchronous collisions with the moving (traveling) nanotube walls. Figure 1 demonstrates the nanopumping effect for 256 He atoms (red) placed inside a L=100 Å long carbon nanotube (carbon atoms are shown in gray color), with a diameter of 12 Å. The nanotube has chirality of (15×0) and was built of 1,410 carbon atoms. After activating the surface traveling wave, with a frequency of 10 THz and a phase velocity of 22 km/s, the helium atoms started to move in the direction of the

wave propagation (in Fig. 1, from left to right). Various instants are shown from an initial 44 fs (Fig.1a), to a final 18 ps (Fig. 1e).

Figure 2a show atomic fluxes generated by the nanopumping effect for various frequencies of the surface waves for the gas initially at rest (<v>=0). The total flux increases up to a few picoseconds and then decreases as a result of the depletion of the gas inside the tube. Average axial velocities of helium atoms are given in Fig. 2b for different wave frequencies. The velocity is small below ~1 THz. At 6 THz the velocity reaches a hyperthermal value of ~30 km/s (the kinetic energy of the atoms is larger $k_B T$). The frequency dependence of the flow rate through the nanopump is given in Fig. 3a; it will depend on the total nanotube length. Since the nanotube length was chosen to be 100 Å, the characteristic frequency is high. The maximum effect is seen at approximately 38 THz. Figure 3b shows the dependence of the nanopumping effect on the ratio L/λ, where λ is the wavelength of the surface wave.

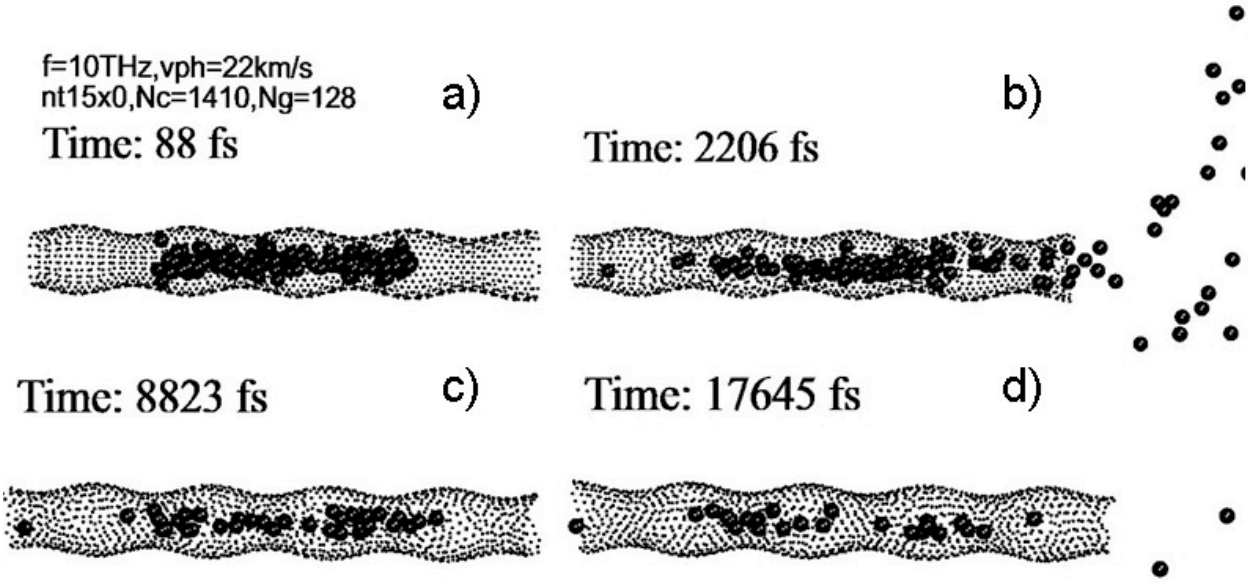

Fig.1. Various instants (from left to right) are shown from an initial 44 fs (Fig. 1a) to final 18 ps (Fig. 1d).

Figure 3 shows our simulation results for the flow rates in three different nanotubes, with the sizes of 50, 100, and 150 Å. Our results show that the flow rate largely depends on the gas density inside the nanotube. In this figure, all nanotubes were filled with the same number of gas atoms, Ng = 256, thus realizing three different gas densities. The density of the gas was three times higher inside the 50 Å nanotube, resulting in a much higher flow rate compared with that of 100 Å and 150 Å nanotubes.

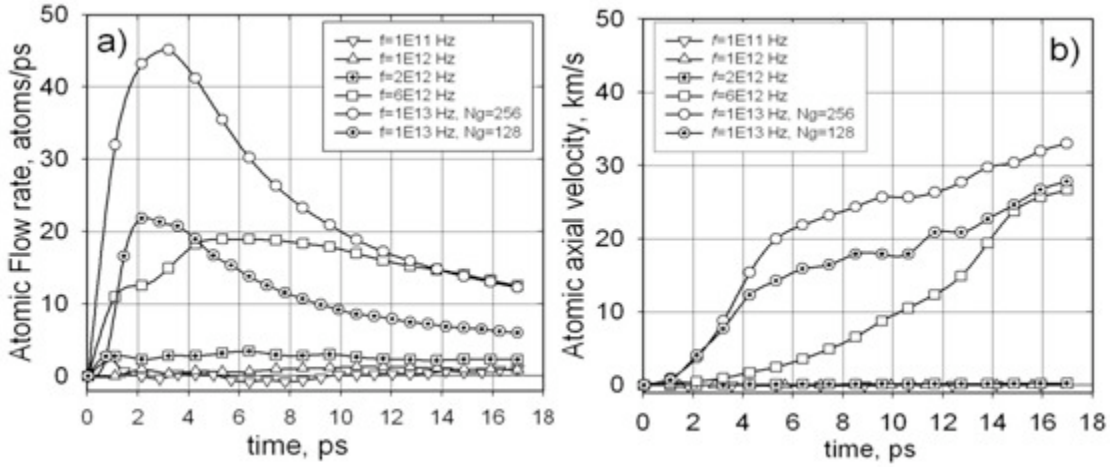

Fig. 2. (a) Dependence of flow rate through the activated nanotubes on the simulation time for various wave frequencies: $10^{11} – 10^{13}$ Hz; (b) average flow velocity vs. time, for various wave frequencies (1 atom/ps = 2.4×10^{-4} sccm).

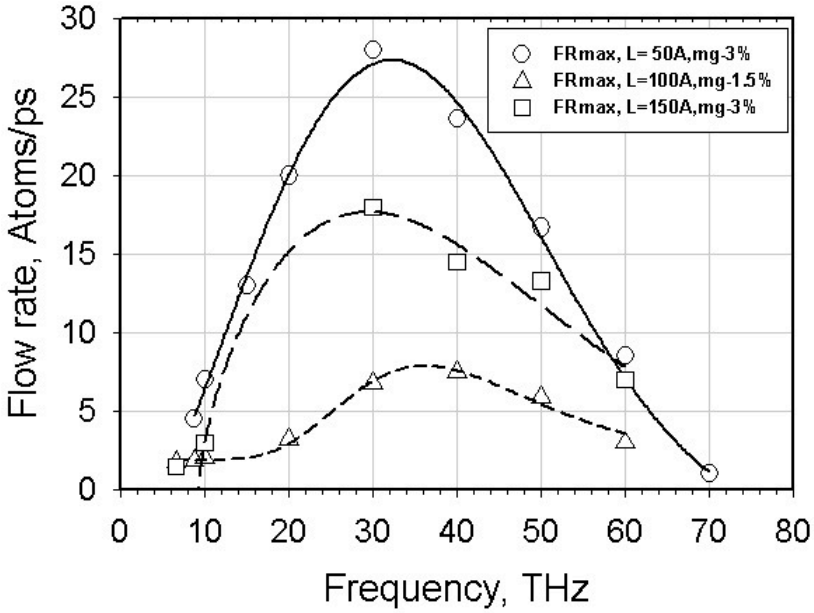

Fig. 3. The dependence of the maximum flow rate on the frequency of the traveling wave for three different nanotube lengths L = 50, 100, and 150Å, for two oscillation magnitudes: 1.5 and 3% of the nanotube radius.

The predicted effect has similarity to real life, for example with the skin features of fast-swimming sea animals, such as dolphins. Some studies indicate that dolphins use specific (traveling) waves on their skin surface to damp the turbulence in the boundary layers near the

skin surface. However, such mechanisms involving compliant surfaces are not yet well understood [43,44].

7. GAS SEPARATION BY ACTIVATED NANOTUBES

A new gas separation effect was demonstrated in our MD simulations. The MD model was applied to various systems containing light gases with different masses less than that of carbon (gas heavier than carbon was able to easily penetrate through the nanotube wall). Some of the preliminary results are shown in Figs. 4 and 5. At the initial time, 128 gas atoms were placed inside the carbon nanotube (64 helium and 64 hydrogen atoms) (Fig. 4a). One can see that after 35 ps of generation of the Rayleigh (traveling) waves, only helium atoms are left inside the nanotube; all hydrogen atoms were pumped out in the direction of the surface waves (from left to right in Fig. 4b). We have found that the separation effect of two gases inside the nanotube is highly selective, depending strongly on the atomic mass of gases and wave frequency.

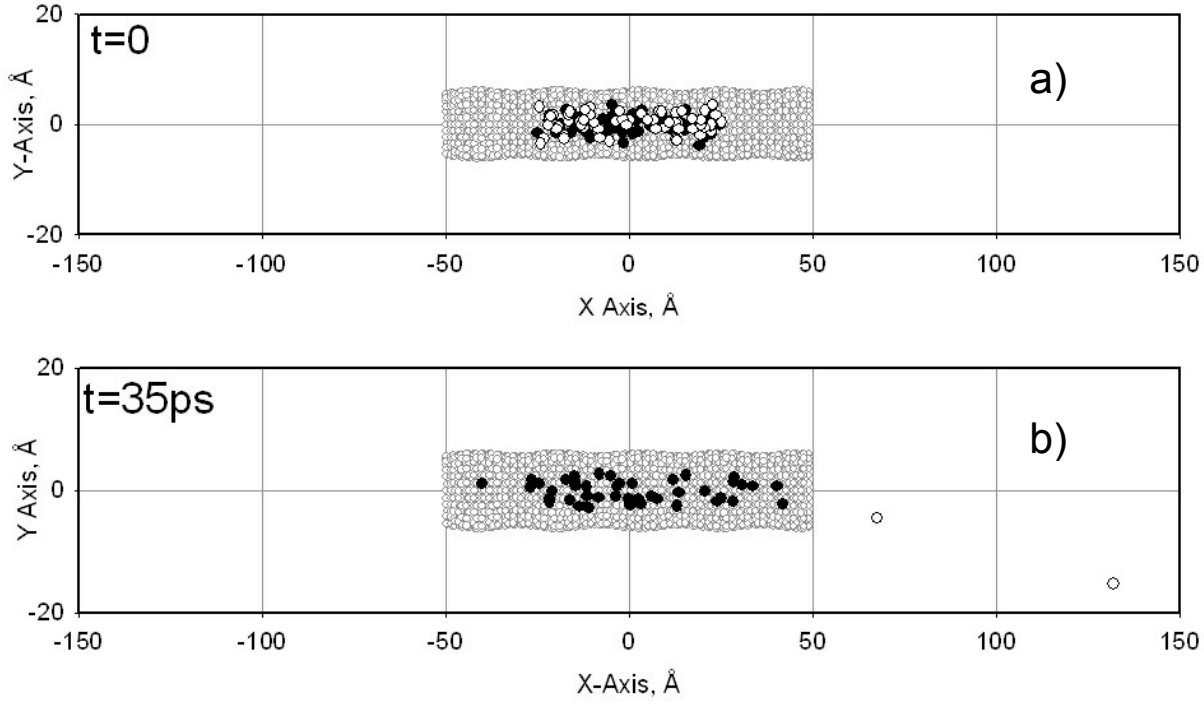

Fig. 4. The gas-separation effect strongly depends on the atomic masses of gases, wave frequency, and phase velocity of the surface wave: (a) the initial position of 128 gas atoms inside the carbon nanotube (64 helium and 64 hydrogen atoms); (b) position after 35 ps of generation of the Rayleigh (traveling) waves on the nanotube surface: only helium atoms are left, and all hydrogen atoms are gone. (The direction of the surface wave is from left to right.)

The gas-separation effect has also been found when the gas is placed outside the

nanotube. Figure 4a shows an initial position of 256 gas atoms outside the carbon nanotube (128 helium and 128 hydrogen atoms); Figure 4b, taken after 140 ps of generation of the Rayleigh (traveling) waves on the nanotube surface, indicates a separation between helium atoms that are mostly moving to the left and hydrogen atoms that are moving to the right.

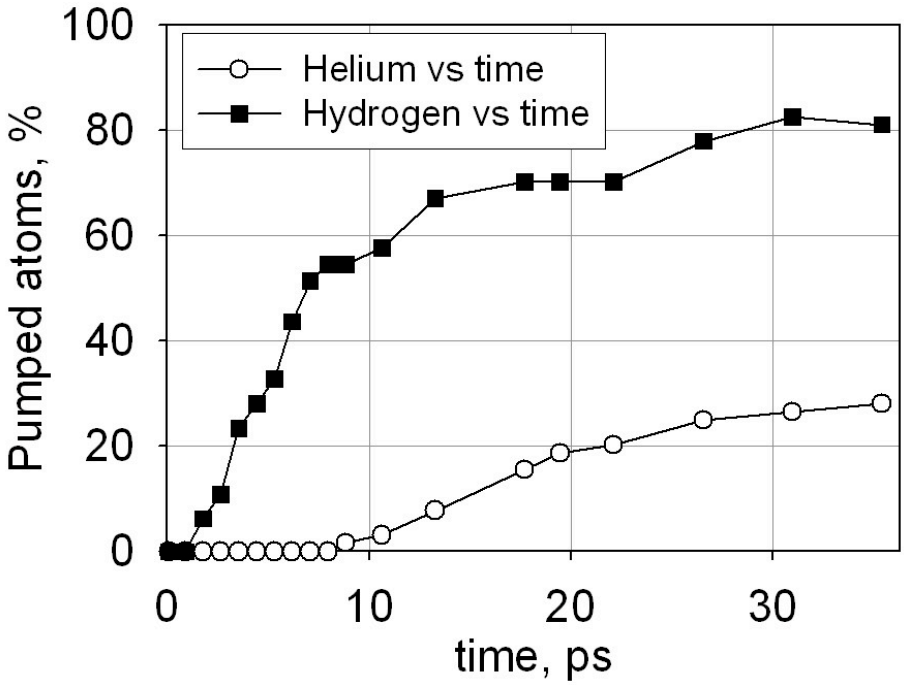

Fig. 5. Number of helium and hydrogen atoms that moved to the right side (the direction of the traveling surface wave) during the nanopumping by activated surface waves on the nanotube surface. Initially, 128 gas atoms were randomly placed inside the {15x0} carbon nanotube (64 helium and 64 hydrogen atoms). After 35 ps of generation of the Rayleigh (traveling) waves on the nanotube surface, almost all the hydrogen atoms were removed by the interaction with the walls, and only helium atoms are left.

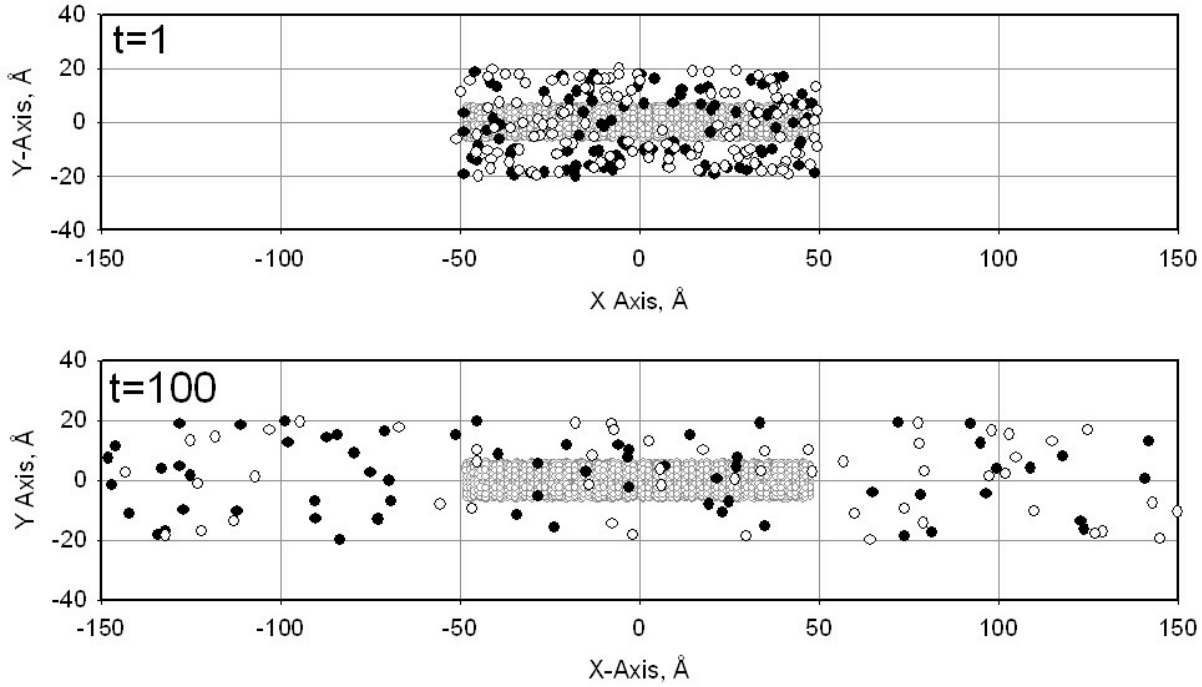

Fig. 6. Gas-separation effect for two gases placed outside the nanotube: (a) initial positions of 256 gas atoms outside the carbon nanotube (128 helium and 128 hydrogen atoms); (b) position after 140 ps of generation of the Rayleigh (traveling) waves on the nanotube surface, showing a separation between them: the helium atoms mostly move to left (opposite direction to the wave movement), and the hydrogen atoms move to right direction (the wave direction).

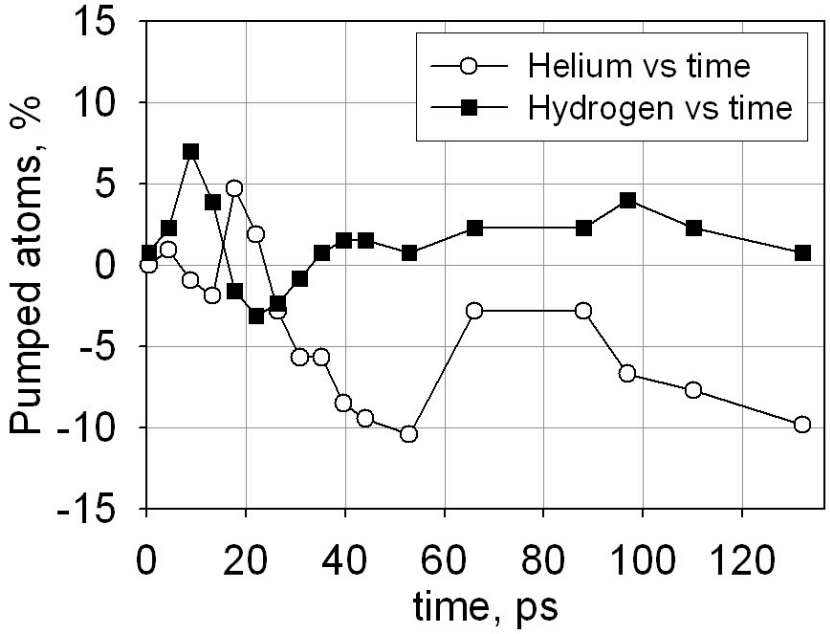

Fig. 7. Weaker gas-separation effect found for two gases placed outside the carbon nanotube. The solid symbols are for the hydrogen full flux in the direction of the wave (from left to right in Fig. 5). The open symbols are for helium atoms showing that helium atoms are moving backward, in opposite direction to the wave movement.

SUMMARY

We have shown that after the Rayleigh (traveling) surface waves are activated on the nanotube surface, the gas inside (or outside) of the carbon nanotube experiences multiple reflections from the nanotube walls. Depending on a combination of the atomic masses, wave frequency, phase velocity, and the relative atomic masses of the gas atoms and carbon, the gas inside the nanotube starts flowing with a macroscopic high velocity, in the direction of the traveling surface wave. We call this "nanopumping."

When a mixture of two or more gases with different atomic masses were placed outside the nanotube, one gas (hydrogen) was flowing in the direction of the Rayleigh waves, but the second gas (helium) was moving in the opposite direction. A similar effect was observed when two gases with different masses were placed inside the nanotube and were separated by applying a surface wave. We call this the "nanoseparation" effect.

The driving force for both effects is the friction between the gas particles and the nanotube walls. Flow rates and the separation rate were calculated at various frequencies and phase velocities of the surface waves. We believe that similar effects should exist for larger space and time scales.

Acknowledgments

This work was supported by the U.S. Department of Energy under Contract No. DE-AC02-06CH11357.

REFERENCES

[1] A.C. Dillon, K.M. Jones, T.A. Bekkedahl, C.H. Kiang, D.S. Bethune and M.J. Heben, *Nature* 386 (1997) 377.
[2] C. Liu, Y.Y. Fan, M. Liu, H.T. Cong, H.M. Cheng and M.S. Dresselhaus, Science 286 (5442) (1999) 1127-1129.
[3] P. Chen, X. Wu, J. Lin, K.L Tan, Science 285 (1999) 91-92.
[4] Y. Ye, C.C. Ahn, C. Witham, B. Fultz, J. Liu, A.G. Rinzler, D. Colbert, K.A. Smith, R.E. Smalley, Appl. Phys. Lett. 74 (1999) 2307.
[5] A.C. Dillon, T. Gennet, J.L. Alleman, K.M. Jones, P.A. Parilla, M.J. Heben: *in Proc. 2000 US DOE Hydrogen Program Review* (2000).
[6] A.C. Dillon, M.J. Heben, Appl. Phys. A72 (2001) 133-142.
[7] V. Meregalli and M. Parinello, Appl. Phys. A 72(2) (2001) 129-132.
[8] J. Li, T. Furuta, H. Goto, T. Ohashi, Y. Fujiwara, S. Yip, *Journ. Chem. Phys.* 119 (2003) 2376-2385.
[9] A. Zuttel, Ch. Nutzenadel, P. Sudan, Ph. Mauron, Ch. Emmenegger, S. Rentsch, L. Schlapbach, A. Weidenkaff, T. Kiyobayashi, J. Alloys Compd. 330–332 (2002) 676.
[10] L. Schlapbach and A. Zuttel, Nature (London) 414 (2001) 353.

[11] Hydrogen, Fuel Cells & Infrastructure Technologies Program Multi-Year Research, Development and Demonstration Plan, February 2005.
http://www1.eere.energy.gov/hydrogenandfuelcells/mypp/
[12]. A.A. Darhuber, S.M. Troian, Annu. Rev. Fluid Mech. 37 (2005) 425.
[13]. J.L. Barrat, L. Bocquet, Faraday Discuss. 112 (1999) 119.
[14]. P.A. Thompson, , S.N. Troian, Nature (London) 389 (1997) 360.
[15]. N.V. Priezjev, , S.M. Troian, Phys. Rev. Lett. 92, 018302 (2004).
[16]. T. Thorsen, , S.J. Maerkl, S.R. Quake, *Science* 298, 580 (2002).
[17]. I. Bitsanis, J.J. Magda, M. Tirrel, H.T. Davis, J. Chem. Phys. 87 (1987) 1733.
[18]. R. Zengerle, M. Richter, J. Micromech. Microeng. 4, 192 (1994).
[19]. M.W.J. Prins, W.J.J. Welters, J.W. Weekamp, Science 291 (2001) 277.
[20]. R.E. Tuzun, D.W. Noid, B.G. Sumpter, R.C. Merkle, Nanotechnology 7 (1996) 241.
[21]. B. Ni, S.B. Sinnot, P.T. Mikulski, J.A. Harrison, Phys. Rev. Lett. 88 (2002) 205505.
[22]. S. Supple, N. Quirke, Phys. Rev. Lett. 90 (2003) 214501.
[23]. S. Supple, N. Quirke, Journ. Chem. Phys. 121 (2004) 214501.
[24]. H.W. Zhang, Z.Q. Zhang, L. Wang, Y.G. Zheng, J.B. Wang, Z.K. Wang, Appl. Phys. Lett. 90 (2007) 144105.
[25]. R. Fan, R. Karnik, M. Yue, D. Li, A. Majumdar, P. Yang, Nano Lett. 5 (2005) 1633.
[26]. P. Kral, D. Tomanek, D. Phys. Rev. Lett. 82 (1999) 5373.
[27]. K. Svensson, H. Olin, E. Olsson, Phys. Rev. Lett. 93 (2004) 145901.
[28]. G. Stan, M.W. Cole, Surf. Sci. 395, 280 (1998).
[29]. V.V. Simonyan, J.K. Johnson, J. Alloys and Comp. 330-332 (2002) 654.
[30]. Y. Zhao, Y.-H. Kim, A.C. Dillon, M.J. Heben, S.B. Zhang, , Phys. Rev. Lett. 94 (2005) 155504.
[31]. M. Hirscher, M. Becher, M. Haluska, F. von Zeppelin, X. Chen, U. Dettlaff-Welikogowska, S.J. Roth, Alloys and Comp., 356-357 (2003) 433.
[32]. A.I. Skoulidas, D.M. Ackerman, J.K. Johnson, D.S. Sholl, Phys. Rev. Lett. 89 (2002) 185901.
[33]. P. Clausing, Ann. Phys. 12 (1932) 961 (English translation: 1971, J. Vac. Sci. Techn. 8, 636).
[34]. Y. Sone, Y. Waniguchi, K. Aoki, Phys. Fluids 8 (1996) 2227.
[35]. A.L. Lereu, A. Passian, R.J. Warmack, T.L. Ferrell, T. Thundat, Appl. Phys. Lett. 84 (2004) 1013.
[36]. N.K. Gupta, Y.B. Gianchandani, Appl. Phys. Lett. 93 (2008) 193511.
[37]. D. Clorennec, D. Royer, Appl. Phys. Lett. 82 (2003) 4608.
[37]. T. Natsuki, T. Hayashi, M. Endo, J. Appl. Phys. 97 (2005) 044307.
[39]. Y. Tsukahara, N. Nakaso, H. Cho, K. Yamanaka, Appl. Phys. Lett. 77 (2000) 2926.
[40]. D. Clorennec, D. Royer, H. Walaszek, Ultrasonics 40 (2002) 783.
[41]. K.L. Telschow, V.A. Deason, D.L. Cottle, J.D. Larson III, Proc. IEEE Ultras. Symp., Puerto Rico, Oct 22-25 (2000).
[42]. I.A. Viktorov, Rayleigh and Lamb Waves: Physical Theory and Applications, Plenum, New York (1967).
[43]. D.P. Hwang, NASA Techn. Memo. 107315, AIAA-97-0546 (1997).
[44]. P.W. Carpenter, C. Davies, A.D. Lucey, Current Sci. 79 (2006) 758.
[45]. Z. Insepov, D. Wolf, A. Hassanein, Nano Lett. 6 (2006) 1893.

[46] Z. Insepov, New nanopumping effect with carbon nanotubes, In Recent Developments in Modeling of Carbon Nanotubes, edited by Q. Wang, B.I. Yakobson, and K.M. Liew, 2009, pp. 1-14 ISBN: 978-81-7895-429-5.
[47] X. Wang, Y. Liu, D. Zhu, Controlled growth of well-aligned carbon nanotubes with large diameters, Chem. Phys. Lett., 340 (2001) 419-424.
[48] Q. Yang, C. Xiao, W. Chen, A. Hirose, Selective growth of diamond and carbon nanostructures by hot filament chemical vapor deposition, Diamond and Rel. Mater. 13 (2004) 433-437.